Chapter 7

Development of Naproxen-like Analogues from Santonin, a Sesquiterpene Lactone

7 Development of Naproxen-like Analogues from Santonin, a Sesquiterpene Lactone

7.1 Introduction

Nature is a treasure of natural molecules with numerous biological potentials, including anti-inflammatory properties. SLs are plant-derived secondary metabolites with anti-inflammatory and other pharmacological potentials [27]. Their structure features the α-methylene-γ-lactone ring, which is postulated to be responsible for their diverse pharmacological activities. SLs are prevalent in various plant families and have anti-inflammatory activity through the inhibition of the NF-kB pathway, COX-2 receptor, NO production, and TNF-α activity [163]. Examples of SLs with reported anti-inflammatory activity include costunolide, parthenolide, cynaropicrin, and micheliolide [29, 163, 169]. Identification of santonin as potential anti-inflammatory SL with COX-2 inhibition as potential target from network pharmacology approach and earlier reports of naproxen-like santonin derivative (**1)** as a new COX-2 antagonist via semi-synthetic modifications, motivated us to synthesize new derivatives [221]. **1** showed good antagonistic activity for COX-2 but not selectivity. Here, we describe our further optimization study of lead **1** to develop more promising COX-2 antagonists.

7.2 Experimental section

7.2.1 General experimental procedure

All chemicals were obtained from Sigma-Aldrich Company and used as received. 1H and 13C NMR spectra were recorded on Bruker-Avance DPX FT-NMR 500 MHz instruments. Chemical data for protons are reported in ppm downfield from TMS and are referenced to the residual proton in the NMR solvent ($CDCl_3$, 7.26 ppm). 13C NMR were recorded at 125 MHz; chemical data for carbons are reported in ppm downfield from

TMS and are referenced to the carbon resonance of the solvent ($CDCl_3$, 77 ppm). HRMS spectra were recorded on HRMS-6540-UHD machines. General method of synthesis

7.2.1.1 General procedure for compounds synthesized in scheme I

Santonin (1 mmol, 245 mg) and iodine (2-3 mmol) were added to a mixture of toluene-methanol solvent system (9:1, 5 mL). The reaction mixture was refluxed at 120 ℃ for 6 hr and the reaction was TLC monitored. An additional portion of iodine was added when required. After completion, the reaction was quenched by adding H_2O containing sodium thiosulfate and partitioned with EtOAc. The organic layer was collected, washed frequently with H_2O, dried over anhydrous Na_2SO_4, and evaporated under vacuum. The resultant product was purified using silica gel chromatography to yield pure analog [221].

2-(7-hydroxy-5,8-dimethyl-1,2,3,4-tetrahydronaphthalen-2-yl)propanoic acid (**1**): 1H NMR (500 MHz, $CDCl_3$) δ 7.89 (d, J = 10.8 Hz, 1H), 7.82 (s, 1H), 7.37 (dd, J = 8.6, 1.8 Hz, 1H), 6.89 (s, 1H), 3.95 (q, J = 7.2 Hz, 1H), 2.59 (s, 3H), 2.48 (s, 3H), 1.64 (d, J = 7.2 Hz, 3H). 13C NMR (126 MHz, $CDCl_3$) δ 180.5, 150.4, 137.4, 134.2, 133.7, 127.7, 125.2, 122.5, 118.5, 113.1, 113.0, 45.8, 19.2, 18.3, 10.3. HRMS *m/z*: $[M+2H]^+$ calc. 246.1245, obs. 246.1199.

2-(7-hydroxy-5,8-dimethylnaphthalen-2-yl)propanoic acid (**2**): 1H NMR (500 MHz, $CDCl_3$) δ 6.54 (s, 1H), 2.86 – 2.70 (m, 4H), 2.61 – 2.50 (m, 4H), 2.48 – 2.32 (m, 3H), 2.17 (s, 6H), 2.12 (d, J = 11.1 Hz, 5H), 2.09 – 1.95 (m, 4H), 1.53 – 1.39 (m, 2H), 1.31 (dd, J = 7.0, 2.6 Hz, 6H). 13C NMR (126 MHz, $CDCl_3$) δ 181.9, 150.9, 135.7, 135.6, 134.4, 134.3, 127.3, 127.2, 119.2, 119.1, 114.3, 114.3, 44.7, 44.2, 37.0, 36.9, 32.0, 30.9, 29.7, 27.2, 26.7, 26.6, 25.5, 19.4, 14.0, 13.8, 10.8, 10.8. HRMS m/z: $[2M+K]^+$ calc. 535.2456, obs. 535.2292. HRMS *m/z*: $[2M+Na]^+$ calc. 519.2717, obs. 519.2588.

7.2.1.2 General procedure for compounds synthesized in scheme II

The derivatives in Scheme II were synthesized by adding santonin (1 mmol, 245 mg) and iodine (2-3 mmol) in a mixture of toluene-alcohol solvent system (8:2 ratio, 5 mL). The alcohols used included methanol, ethanol, 1-propanol, 1-butanol, 1-pentanol, 1-hexanol, 1-heptanol, 1-octanol, and isoamyl alcohol. The reaction mixture was refluxed at 120 ℃ for 12 hr and was TLC monitored. An additional portion of iodine was added when required. After completion, the reaction was quenched by adding H_2O containing sodium thiosulfate and partitioned with EtOAc. The organic layer was collected, washed frequently with H_2O, dried over anhydrous Na_2SO_4, and evaporated under a vacuum. The product was purified using silica gel chromatography to yield pure analogs.

Methyl 2-(7-methoxy-5,8-dimethylnaphthalen-2-yl)propanoate (3): 1H NMR (500 MHz, $CDCl_3$) δ 7.94 (d, J = 8.7 Hz, 1H), 7.87 (s, 1H), 7.39 (dd, J = 8.7, 2.0 Hz, 1H), 7.13 (s, 1H), 3.96 (s, 4H), 3.71 (s, 3H), 2.71 (s, 3H), 2.56 (s, 3H), 1.64 (d, J = 7.2 Hz, 3H). 13C NMR (500 MHz, $CDCl_3$) δ 175.1, 154.3, 138.1, 134.0, 133.4, 127.4, 125.1, 122.9, 122.5, 117.2, 114.9, 56.8, 52.1, 45.9, 19.7, 18.7, 10.4. HRMS *m/z*: $[M+H]^+$ calc. 273.1485, obs. 273.1433.

Ethyl 2-(7-ethoxy-5,8-dimethylnaphthalen-2-yl)propanoate (4): 1H NMR (500 MHz, $CDCl_3$) δ 7.95 (d, J = 10.2 Hz, 1H), 7.89 (s, 1H), 7.41 (dd, J = 8.6, 1.8 Hz, 1H), 7.12 (s, 1H), 4.27 – 4.11 (m, 4H), 3.94 (q, J = 7.2 Hz, 1H), 2.70 (s, 3H), 2.59 (s, 3H), 1.65 (dd, J = 7.1, 1.9 Hz, 3H), 1.49 (td, J = 6.9, 1.1 Hz, 3H), 1.26 (td, J = 7.1, 1.4 Hz, 3H). 13C NMR (500 MHz, $CDCl_3$) δ 174.7, 153.6, 138.2, 134.1, 133.3, 127.5, 124.9, 122.8, 122.6, 117.9, 116.6, 65.5, 60.8, 46.1, 19.6, 18.8, 15.4, 14.2, 10.6. HRMS *m/z*: $[M+H]^+$ calc. 301.1798, obs. 301.1751.

Propyl 2-(7-propoxy-5,8-dimethylnaphthalen-2-yl)propanoate (5): 1H NMR (500 MHz, $CDCl_3$) δ 7.92 (d, J = 8.7 Hz, 1H), 7.86 (s, 1H), 7.38 (dd, J = 8.7, 1.8 Hz, 1H), 7.10

(s, 1H), 4.06 (td, *J* = 6.6, 3.9 Hz, 3H), 3.93 (q, *J* = 7.2 Hz, 1H), 2.68 (s, 3H), 2.56 (s, 3H), 1.91-1.84 (m, 2H), 1.66 – 1.58 (m, 5H), 1.11 (t, *J* = 7.4 Hz, 3H), 0.89 (t, *J* = 7.4 Hz, 3H). 13C NMR (500 MHz, $CDCl_3$) *δ* 174.8, 153.7, 138.1, 134.1, 133.2, 127.4, 124.9, 122.8, 122.5, 117.8, 116.4, 71.5, 66.4, 46.1, 23.1, 21.9, 19.6, 18.7, 10.7, 10.5, 10.3. HRMS *m/z*: $[M+H]^+$ calc. 329.2111, obs. 329.2124.

Butyl 2-(7-butoxy-5,8-dimethylnaphthalen-2-yl)propanoate (6): 1H NMR (500 MHz, $CDCl_3$) *δ* 7.92 (d, *J* = 8.6 Hz, 1H), 7.86 (s, 1H), 7.38 (dd, *J* = 8.7, 1.8 Hz, 1H), 7.10 (s, 1H), 4.11 (td, *J* = 6.6, 1.6 Hz, 4H), 3.93 (q, *J* = 7.2 Hz, 1H), 2.69 (s, 3H), 2.56 (s, 3H), 1.89 – 1.80 (m, 2H), 1.66 – 1.56 (m, 7H), 1.39 – 1.28 (m, 2H), 1.03 (t, *J* = 7.4 Hz, 3H), 0.90 (t, *J* = 7.4 Hz, 3H). 13C NMR (500 MHz, $CDCl_3$) *δ* 174.7, 153.8, 138.1, 134.1, 133.2, 127.4, 124.9, 122.8, 122.5, 117.8, 116.3, 69.6, 64.6, 46.1, 31.9, 30.6, 19.6, 19.4, 19.1, 18.7, 13.9, 13.6, 10.5. HRMS *m/z*: $[M+H]^+$ calc. 357.2424, obs. 357.2419.

Pentyl 2-(7-pentyloxy-5,8-dimethylnaphthalen-2-yl)propanoate (7): 1H NMR (500 MHz, $CDCl_3$) *δ* 7.92 (d, *J* = 8.7 Hz, 1H), 7.87 (d, *J* = 1.8 Hz, 1H), 7.39 (dd, *J* = 8.7, 1.8 Hz, 1H), 7.10 (s, 1H), 4.13 – 4.07 (m, 4H), 3.93 (q, *J* = 7.2 Hz, 1H), 2.69 (s, 3H), 2.56 (s, 3H), 1.90 – 1.82 (m, 2H), 1.64-1.58 (m, 5H), 1.55 – 1.49 (m, 2H), 1.48 – 1.42 (m, 2H), 1.31 – 1.24 (m, 4H), 0.98 (t, *J* = 7.3 Hz, 3H), 0.85 (t, *J* = 6.9 Hz, 3H). 13C NMR (126 MHz, $CDCl_3$) *δ* 174.8, 153.8, 138.1, 134.1, 133.2, 127.4, 124.9, 122.8, 122.6, 117.7, 116.4, 69.9, 64.9, 46.1, 29.5, 28.4, 28.3, 27.9, 22.5, 22.3, 19.6, 18.7, 14.1, 13.9, 10.5. HRMS *m/z*: $[M+H]^+$ calc. 385.2737, obs. 385.2744.

Hexyl 2-(7-hexyloxy-5,8-dimethylnaphthalen-2-yl)propanoate (8): 1H NMR (500 MHz, $CDCl_3$) *δ* 7.92 (d, *J* = 8.7 Hz, 1H), 7.86 (s, 1H), 7.38 (dd, *J* = 8.7, 1.7 Hz, 1H), 7.10 (s, 1H), 4.10 (td, *J* = 7.2, 2.6 Hz, 4H), 3.93 (q, *J* = 7.2 Hz, 1H), 2.68 (s, 3H), 2.56 (s, 3H), 1.90 – 1.79 (m, 2H), 1.65 – 1.56 (m, 5H), 1.42 – 1.22 (m, 12H), 0.98 – 0.82 (m, 6H). 13C NMR (500 MHz, $CDCl_3$) *δ* 174.8, 153.8, 138.1, 134.1, 133.2, 127.4, 124.9, 122.8, 122.6,

117.7, 116.4, 69.9, 64.9, 46.1, 31.6, 31.4, 29.7, 28.5, 25.8, 25.5, 22.7, 22.5, 19.6, 18.7, 14.1, 13.9, 10.5. HRMS *m/z*: $[M+H]^+$ calc. 413.3050, obs. 413.3064.

Heptyl 2-(7-heptyloxy-5,8-dimethylnaphthalen-2-yl) propanoate (9): 1H NMR (500 MHz, $CDCl_3$) δ 7.90 (d, J = 8.7 Hz, 1H), 7.84 (s, 1H), 7.36 (dd, J = 8.7, 1.8 Hz, 1H), 7.08 (s, 1H), 4.08 (td, J = 6.6, 3.2 Hz, 4H), 3.91 (q, J = 7.1 Hz, 1H), 2.66 (s, 3H), 2.54 (s, 3H), 1.88 – 1.77 (m, 2H), 1.64 – 1.46 (m, 8H), 1.42 – 1.29 (m, 7H), 1.28 – 1.20 (m, 6H), 0.88 (dt, J = 35.9, 7.1 Hz, 6H). 13C NMR (500 MHz, $CDCl_3$) δ 174.8, 153.8, 138.1, 134.1, 133.2, 127.4, 124.9, 122.8, 122.5, 117.7, 116.3, 69.9, 64.9, 46.1, 31.9, 31.7, 29.8, 29.1, 28.9, 28.6, 26.1, 25.8, 22.7, 22.5, 19.6, 18.7, 14.1, 14.1, 10.5. HRMS *m/z*: $[M+H]^+$ calc. 441.3363, obs. 441,3374.

Octyl 2-(7-octyloxy-5,8-dimethylnaphthalen-2-yl) propanoate (**10**)**:** 1H NMR (500 MHz, $CDCl_3$) δ 7.92 (d, J = 8.6 Hz, 1H), 7.87 (s, 1H), 7.39 (dd, J = 8.6, 1.9 Hz, 1H), 7.10 (s, 1H), 4.10 (td, J = 6.7, 3.9 Hz, 4H), 3.93 (q, J = 7.0 Hz, 1H), 2.69 (s, 3H), 2.56 (s, 3H), 1.85 (q, J = 7.8 Hz, 2H), 1.66 – 1.57 (m, 5H), 1.40 – 1.19 (m, 20H), 0.90 (m, 6H). 13C NMR (500 MHz, $CDCl_3$) δ 174.7, 153.8, 138.1, 134.1, 133.2, 127.4, 124.9, 122.8, 122.5, 117.7, 116.4, 69.9, 64.9, 46.1, 31.8, 31.7, 29.9, 29.4, 29.3, 29.1, 29.1, 28.6, 26.2, 25.8, 22.7, 22.6, 19.6, 18.7, 14.1, 14.1, 10.5. HRMS *m/z*: $[M+H]^+$ calc. 469.3676, obs. 469.3663.

Isopentyl 2-(7-isopentyloxy-5,8-dimethylnaphthalen-2-yl) propanoate (11): 1H NMR (500 MHz, $CDCl_3$) δ 7.92 (d, J = 8.7 Hz, 1H), 7.85 (s, 1H), 7.37 (d, J = 9.6 Hz, 1H), 7.11 (s, 1H), 4.13 (q, J = 7.4 Hz, 4H), 3.92 (q, J = 6.9 Hz, 1H), 2.69 (s, 3H), 2.55 (s, 3H), 1.81-1.71 (m, 2H), 1.71 – 1.54 (m, 5H), 1.53-1.46 (m, 2H), 1.04-0.97 (m, 6H), 0.94 – 0.78 (m, 6H). 13C NMR (500 MHz, $CDCl_3$) δ 174.7, 153.8, 138.1, 134.1, 133.2, 127.4, 124.9, 122.8, 122.5, 117.7, 116.2, 68.2, 63.5, 46.1, 38.8, 37.3, 26.2, 25.1, 22.6, 22.4, 19.6, 18.7, 10.5. HRMS *m/z*: $[M+H]^+$ calc. 385.2737, obs. 385.2746.

7.2.1.3 General procedure for compounds synthesized in scheme III

The derivatives synthesized in Scheme II were hydrolyzed by adding the synthesized compound (1 mmol) in a mixture containing 1N methanolic NaOH (5 ml) and DCM (5 ml). The reaction mixture was stirred at room temperature for 2 hours and was TLC monitored. After the completion of the reaction, the reaction mixture was neutralized by adding dilute HCl and extracted with EtOAc (3-4 times). The organic layer was collected, dried over anhydrous Na_2SO_4, and evaporated under a vacuum. The resultant product was purified using silica gel chromatography to yield pure analog.

2-(7-methoxy-5,8-dimethylnaphthalen-2-yl) propanoic acid (12): 1H NMR (500 MHz, $CDCl_3$) δ 7.94 (d, J = 8.7 Hz, 1H), 7.88 (s, 1H), 7.39 (dd, J = 8.7, 1.8 Hz, 1H), 7.12 (s, 1H), 3.95 (s, 4H), 2.69 (s, 3H), 2.54 (s, 3H), 1.64 (d, J = 7.2 Hz, 3H). 13C NMR (500 MHz, $CDCl_3$) δ 180.3, 154.3, 137.2, 133.9, 133.4, 127.5, 125.1, 122.9, 122.7, 117.3, 115.1, 56.9, 45.8, 19.7, 18.3, 10.4. HRMS *m/z*: $[M+H]^+$ calc. 259.1329, obs. 259.1334 (Appendix, Figure A.36-A.38).

2-(7-ethoxy-5,8-dimethylnaphthalen-2-yl) propanoic acid (13): 1H NMR (500 MHz, $CDCl_3$) δ 7.93 (d, J = 8.6 Hz, 1H), 7.88 (s, 1H), 7.39 (dd, J = 8.6, 2.1 Hz, 1H), 7.10 (s, 1H), 4.06 (t, J = 6.5 Hz, 2H), 3.95 (q, J = 7.2 Hz, 1H), 2.67 (s, 3H), 2.55 (s, 3H), 1.64 (d, J = 7.3 Hz, 3H), 1.11 (t, J = 7.4 Hz, 3H). 13C NMR (500 MHz, $CDCl_3$) δ 153.8, 137.2, 134.1, 133.3, 127.6, 125.1, 122.8, 122.6, 117.8, 116.6, 71.5, 45.7, 23.1, 19.6, 18.3, 10.7, 10.5. HRMS *m/z*: $[M+H]^+$ calc. 273.1485, obs. 273.1425.

2-(7-propoxy-5,8-dimethylnaphthalen-2-yl) propanoic acid (14): 1H NMR (500 MHz, $CDCl_3$) δ 7.95 (d, J = 8.6 Hz, 1H), 7.91 (s, 1H), 7.42 (dd, J = 8.7, 2.0 Hz, 1H), 7.12 (s, 1H), 4.18 (q, J = 7.0 Hz, 2H), 3.98 (d, J = 7.2 Hz, 1H), 2.69 (s, 3H), 2.57 (s, 3H), 2.26 (dd, J = 15.7, 2.6 Hz, 2H), 1.66 (d, J = 7.2 Hz, 3H), 1.49 (t, J = 7.0 Hz, 3H). 13C NMR (500 MHz, $CDCl_3$) δ 180.9, 153.8, 137.3, 134.2, 133.4, 127.8, 125.7, 125.2, 123.1, 118.2,

116.9, 65.6, 45.9, 24.5, 19.7, 18.4, 15.4, 10.7. HRMS *m/z*: $[M+H]^+$ calc. 287.1642, obs. 287.1583.

2-(7-butoxy-5,8-dimethylnaphthalen-2-yl) propanoic acid (15): 1H NMR (500 MHz, $CDCl_3$) δ 7.94 (d, *J* = 8.7 Hz, 1H), 7.89 (s, 1H), 7.40 (dd, *J* = 8.7, 1.8 Hz, 1H), 7.11 (s, 1H), 4.11 (t, *J* = 6.5 Hz, 2H), 3.96 (q, *J* = 7.1 Hz, 1H), 2.69 (s, 3H), 2.56 (s, 3H), 1.89 – 1.79 (m, 2H), 1.65 (d, *J* = 7.2 Hz, 3H), 1.62-1.52 (m, 2H), 1.04 (t, *J* = 7.4 Hz, 3H). 13C NMR (500 MHz, $CDCl_3$) δ 180.7, 153.8, 137.2, 134.1, 133.3, 127.6, 125.1, 122.9, 122.6, 117.8, 116.5, 69.6, 45.8, 31.9, 19.6, 19.4, 18.3, 13.9, 10.5. HRMS *m/z*: $[M+H]^+$ calc. 301.1798, obs. 301.1819.

2-(7-pentyloxy-5,8-dimethylnaphthalen-2-yl) propanoic acid (16): 1H NMR (500 MHz, $CDCl_3$) δ 7.95 (d, *J* = 8.7 Hz, 1H), 7.90 (s, 1H), 7.41 (dd, *J* = 8.7, 1.8 Hz, 1H), 7.12 (s, 1H), 4.11 (t, *J* = 6.5 Hz, 2H), 3.98 (q, *J* = 7.2 Hz, 1H), 2.70 (s, 3H), 2.58 (s, 3H), 1.92 – 1.79 (m, 2H), 1.66 (d, *J* = 7.2 Hz, 3H), 1.59 – 1.51 (m, 2H), 1.50 – 1.40 (m, 2H), 1.00 (t, *J* = 7.3 Hz, 3H). 13C NMR (500 MHz, $CDCl_3$) δ 180.6, 153.7, 137.0, 133.9, 133.1, 127.4, 124.9, 122.7, 122.5, 117.7, 116.4, 69.8, 45.7, 29.3, 28.2, 22.4, 19.5, 18.1, 13.9, 10.4. HRMS *m/z*: $[M+H]^+$ calc. 315.1955, obs. 315.1892.

2-(7-hexyloxy-5,8-dimethylnaphthalen-2-yl) propanoic acid (17): 1H NMR (500 MHz, $CDCl_3$) δ 7.93 (d, *J* = 8.7 Hz, 1H), 7.88 (s, 1H), 7.39 (dd, *J* = 8.7, 1.8 Hz, 1H), 7.10 (s, 1H), 4.09 (t, *J* = 6.5 Hz, 2H), 3.95 (q, *J* = 7.2 Hz, 1H), 2.67 (s, 3H), 2.55 (s, 3H), 1.89 – 1.78 (m, 2H), 1.64 (d, *J* = 7.2 Hz, 3H), 1.59 – 1.48 (m, 2H), 1.44-1.31 (m, 4H), 0.95 (t, *J* = 7.1 Hz, 3H). 13C NMR (500 MHz, $CDCl_3$) δ 180.4, 153.9, 137.5, 134.2, 133.4, 127.7, 125.2, 122.9, 122.8, 117.9, 116.5, 69.9, 46.0, 31.8, 29.9, 25.9, 22.8, 19.7, 18.4, 14.2, 10.6. HRMS *m/z*: $[M+H]^+$ calc. 329.2111, obs. 329.2045.

2-(7-heptyloxy-5,8-dimethylnaphthalen-2-yl) propanoic acid (18): 1H NMR (500 MHz, $CDCl_3$) δ 7.93 (d, *J* = 8.7 Hz, 1H), 7.87 (s, 1H), 7.39 (dd, *J* = 8.7, 2.0 Hz, 1H), 7.10

(s, 1H), 4.08 (t, *J* = 6.5 Hz, 2H), 3.96 (q, *J* = 7.3 Hz, 1H), 2.67 (s, 3H), 2.54 (s, 3H), 1.96 – 1.75 (m, 2H), 1.64 (d, *J* = 7.2 Hz, 3H), 1.58-1.46 (m, 2H), 1.40-1.28 (m, 6H), 0.92 (t, *J* = 6.8 Hz, 3H). 13C NMR (500 MHz, $CDCl_3$) *δ* 180.5, 153.9, 137.2, 134.1, 133.2, 127.6, 125.1, 122.9, 122.6, 117.8, 116.6, 69.9, 45.8, 31.8, 29.8, 29.1, 26.1, 22.7, 19.6, 18.3, 14.2, 10.5. HRMS *m/z*: $[M+H]^+$ calc. 343.2268, obs. 343.2200.

2-(7-octyloxy-5,8-dimethylnaphthalen-2-yl) propanoic acid (19): 1H NMR (500 MHz, $CDCl_3$) *δ* 7.93 (d, *J* = 8.7 Hz, 1H), 7.89 (s, 1H), 7.39 (dd, *J* = 8.6, 1.8 Hz, 1H), 7.11 (s, 1H), 4.09 (t, *J* = 6.5 Hz, 2H), 3.96 (q, *J* = 7.1 Hz, 1H), 2.68 (s, 3H), 2.56 (s, 3H), 1.90 – 1.81 (m, 2H), 1.65 (d, *J* = 7.2 Hz, 3H), 1.53 (q, *J* = 7.6 Hz, 2H), 1.41 – 1.32 (m, 8H), 0.93 (t, *J* = 6.7 Hz, 3H). 13C NMR (500 MHz, $CDCl_3$) *δ* 180.6, 153.8, 137.1, 134.0, 133.3, 127.6, 125.1, 122.9, 122.6, 117.8, 116. 6, 69.9, 45.8, 31.9, 29.8, 29.4, 29.3, 26.9, 22.7, 19.6, 18.3, 14.1, 10.5. HRMS *m/z*: $[M+3H]^+$ calc. 359.2570, obs. 359.2512.

2-(7-isopentyloxy-5,8-dimethylnaphthalen-2-yl) propanoic acid (20): 1H NMR (500 MHz, CD_3OD) *δ* 7.94 (d, *J* = 8.7 Hz, 1H), 7.90 (s, 1H), 7.41 (dd, *J* = 8.7, 2.1 Hz, 1H), 7.13 (s, 1H), 4.19 – 4.10 (m, 2H), 3.98 (t, *J* = 7.8 Hz, 1H), 2.69 (s, 3H), 2.57 (s, 3H), 1.99 – 1.91 (m, 1H), 1.77 (q, *J* = 6.7 Hz, 2H), 1.66 (d, *J* = 7.2 Hz, 3H), 1.04 (dd, *J* = 6.5, 1.9 Hz, 6H). 13C NMR (126 MHz, CD_3OD) *δ* 180.9, 153.9, 137.3, 134.2, 133.3, 127.6, 125.2, 122.9, 122.7, 117.9, 116.5, 68.3, 45.9, 38.6, 25.2, 22.7, 19.7, 18.4, 10.6. HRMS *m/z*: $[M+H]^+$ calc. 315.1955, obs. 315.1894.

7.2.2 COX inhibition assay

The compounds' ability to inhibit COX-1 and COX-2 was assessed by utilizing a human COX inhibitory screening assay kit (Cayman Chemical, catalog no. 701230) in accordance with the manufacturer's guidelines. The compounds were tested at final concentrations of 10, 100, and 1000 nM. The absorbance was then recorded at 405 nm using a microplate reader from Bio-Rad Laboratories, CA, USA. IC_{50} values were

determined using the sigmoidal dose-response equation (variable slope) via GraphPad software. These experiments were conducted in duplicate.

7.2.3 Docking study

The docking study of **12** was conducted to determine its binding interaction with COX-2 (PDB: 3NT1) protein. The protocol was same as mentioned in Section 4.2.3.2.

7.2.4 MD simulation study

As mentioned in Section 6.2.8.

7.2.5 *In vivo* studies

7.2.5.1 Experimental animals

Male Sprague Dawley rats weighing between 200-250 g were employed for the study. The rats were housed in groups of three per cage under standard conditions, with a temperature maintained at 21 ± 2 °C and a 12-hour light-dark cycle. Animals were provided with ad-libitum access to standard laboratory food and sterile water. All the rats were randomly allocated to the various experimental groups (n=6/group). From here onwards analog **12** will be referred as TC (test compound).

7.2.5.2 Ethical committee approval

All experiments were performed with adherence to the guidelines set forth by the International Association for the Study of Pain and the Committee for the Purpose of Control and Supervision of Experiments on Animals (CPCSEA), Government of India, New Delhi. The experimental protocols were approved by the Institute Animal Ethics Committee of Indian Institute of Technology (Banaras Hindu University), Varanasi, UP, India (**IIT(BHU)/IAEC/2022/059**).

7.2.5.3 Animal model and experimental design

To induce chronic inflammatory pain, rats were administered with 100 µL complete Freund's adjuvant (CFA) through intra-plantar injection. Various pain behavioral assays

were done before and after CFA administration and at different time points post-drug and vehicle administration. Treatment started on day four post-CFA injection with the vehicle, TC (1, 3, and 10 mg/kg i.p.), and naproxen (10 mg/kg i.p.). Behavioral assessments including heat hyperalgesia, cold allodynia and hyperalgesia, and mechanical allodynia and hyperalgesia were conducted both before and after drug treatment. For pain behavior studies, rats were divided into six experimental groups with six rats/group. The first group consists of naïve healthy rats, while the second group was the disease control group where CFA rats were administered with the vehicle of TC. Rats in the third, fourth, and fifth groups belonged to different test groups where CFA rats were treated with intraperitoneal TC at 1 mg/kg, 3 mg/kg, and 10 mg/kg respectively. The sixth group consists of the standard control group in which CFA rats were treated with naproxen (10 mg/kg *i.p*). For open field and rota-rod tests rats were treated with vehicle, TC (10 mg/kg *i.p*), and naproxen (10 mg/kg *i.p*) respectively.

7.2.5.4 Animal behavior tests

7.2.5.4.1 Mechanical allodynia and hyperalgesia test

7.2.5.4.1.1 von-Frey hair test: Mechanical allodynia

The von-Frey hair test was utilized to evaluate mechanical allodynia in rats with CFA-induced inflammation. It involves employing thin filaments with varying forces applied to the plantar surface of the hind paw [222]. Mechanical sensitivity was assessed using von-Frey filaments (Stoelting Co., USA) with different intensities ranging from 0.40 g to 13 gm (0.38, 0.57, 1.23, 1.83, 3.66, 5.93, 9.13, 13.1 g). The paw withdrawal threshold, defined as the minimum pressure (in g) required to elicit paw withdrawal, was recorded. The rats were placed in transparent plexiglass chambers atop wire-mesh plates and allowed to acclimate for 10-15 minutes before testing. The up-down method was employed to assess mechanical sensitivity before and after CFA injection, as well as post-

drug treatment. von-Frey filaments were applied to the footpads of the sub-plantar region of the hind paw from underneath the mesh. Testing began with a 1.8 g force von-Frey filament. If this initial stimulus elicited a positive response, subsequent testing was conducted with finer filaments of lower forces. Conversely, if the initial application did not provoke a response, further testing involved using thicker filaments with higher forces. The test continued until either response to five stimuli were assessed after the first crossing of the withdrawal threshold or the maximum/minimum end of the von-Frey hair set was reached before a positive/negative response was obtained. The paw withdrawal, licking, and shaking in response to the von-Frey filament, was considered as positive response. Pre-injury baseline, as well as 0.5 hr, 1 hr, 2 hr, and 4 hr post-drug/vehicle administration thresholds, were measured in CFA rats [223-225].

7.2.5.4.1.2 Pinprick test: Mechanical hyperalgesia

The pinprick test is a method used to evaluate mechanical hyperalgesia and nociceptive responses in rodents. Rats were acclimated to a wire mesh platform for a duration of 2 to 3 days. A custom-designed pin-prick stimulator was employed to administer the stimulus, involving the attachment of a 22-gauge needle perpendicular to the von-Frey hair. The pin was gently applied to the hind paw of rats to elicit a noxious response, with caution taken to prevent skin puncture. This procedure was repeated 10 times for each hind paw. The number of paw withdrawals during the 10 trials was recorded by an observer blinded to the experiment [225, 226].

7.2.5.4.2 Thermal stimuli pain assays

7.2.5.4.2.1 Hargreaves test: Thermal hyperalgesia

The Hargreaves test is a method employed to assess the signs of heat hypersensitivity in rats that measures paw withdrawal latency (PWL) to radiant heat stimuli [227]. Thermal hyperalgesia was measured in CFA rats using Hargreaves apparatus (Ugo Basile, Italy).

Animals were enclosed in transparent acrylic chambers and allowed to be acclimatized on Hargreaves apparatus. On the test day, an automated movable infrared (IR) beam source was directed precisely to the plantar surface of the hind paw and the cut-off time was set to 20 sec to avoid the tissue damage. The measurements were recorded for both paws of rats, i.e., ipsilateral and contralateral in triplicate. The glass floor was cleaned with 70% ethanol both before and after testing each animal for heat hyperalgesia. All the experimental groups were tested for thermal hyperalgesia pre-injury baseline followed by pre-drug baseline and at different time-points post drug administration [223, 226, 228].

7.2.5.4.3 Cold stimuli pain assay

7.2.5.4.3.1 Ice floor test

The ice floor test is a technique employed to assess nociceptive responses and sensitivity to noxious cold stimuli in rats. During the experiment, the rats were placed in a transparent plexiglass chamber with an ice floor. A temperature sensor was placed on the surface to continuously monitor the temperature changes. The temperature was maintained at 4 °C ± 2 °C for the entire duration of the test. The test was video recorded under moderate illumination for 1 minute, and the lifting of the paws was measured by an observer blinded to the experimental conditions. Pre-injury baseline and 0.5 hr, 1 hr, 2 hr, and 4 hr post-drug/vehicle administration paw lifts were counted in CFA-injected rats [226, 228, 229].

7.2.5.4.3.2 Acetone evaporation test

The acetone drop test is a method used to evaluate cold allodynia and nociceptive responses to non-noxious cold stimuli in rodents. The animals' reactions to acetone were observed and quantified, often in terms of behaviors like paw flicking and licking induced by the cooling sensation produced by acetone at temperatures between 15 to 21 °C. In brief, the rats were acclimatized to plexiglass chambers positioned on top of a von-Frey mesh. To assess cold allodynia, a drop (100 μL) of acetone was carefully applied to the

dorsal area of the hind paw without direct skin contact. The test was video recorded for 1 minute, and scoring was performed by an observer blinded to the experimental conditions. The animal responses were scored using the following scale: 0- No response, 1- Paw flicking, 2- Repeated paw flicking, 3- Repeated paw flicking with licking. The response score was calculated as the average of three trials [224, 225, 230].

7.2.5.4.4 Behavioral neurotoxicity assays

7.2.5.4.4.1 Rota-rod test

Rota-rod test was performed to measure the motor-coordination activity of rats before and after drug treatment. The rats were acclimatized and trained using a rotating rod apparatus (Ugo Basile, Italy). The testing protocol consisted of a training session followed by the actual test. Initially, on day 1, rats underwent training at a speed of 5 revolutions per minute (rpm) for 120 sec. Subsequently, on the testing day, the assessment was carried out at a consistent speed of 25 rpm both before and after drug administration. Rats were allowed to stay on the accelerating rod for a maximum of 120 sec (cut-off time), and the time rats spent on the rod was noted [225, 231].

7.2.5.4.4.2 Open field test

The test was performed to evaluate the effect of the drugs on the locomotor behavior of rats post drug treatment. If the test drug exhibits neurotoxic potential, it might lead to a reduction in locomotor activity, as evidenced by a decrease in parameters such as total distance travelled. Animal habituation was performed one day before the test in order to make the rats familiar with the novel environment. On testing day, rats were placed in the open filed apparatus (45x45x75cm) and the behavior was monitored and video recorded for 10 minutes. The Any Maze software (Version 7.2, Stoelting, USA) equipped with a video tracking system was employed for recording and total distance covered was measured [223, 224].

7.2.5.5 Biochemical analysis

7.2.5.5.1 Tissue harvesting and storage

After the completion of the behavioral studies, the animals were euthanized by administering a high dosage of ketamine and xylazine followed by cervical decapitation. Further for biochemical analysis, the sciatic nerve was isolated through the dissection of biceps femoris muscle. The isolated sciatic nerve was subjected to thorough cleansing with 0.9% normal saline to remove any external contaminants or debris. The sciatic nerve samples were then processed on ice with a hand-held homogenizer, and the homogenized lysate was centrifuged at 12,000 rpm for 20 min at 4 °C. The resulting supernatant (cytosolic fraction), was then collected and stored in aliquots at −80 °C for biochemical analysis [226]. The estimation of oxidative stress markers including GSH, MDA, and nitrite was done using specific assays.

7.2.5.5.2 Lipid peroxidation (LPO) assay

LPO is a process that involves the oxidative degradation of lipids (fats) in cell membranes, resulting in the production of lipid peroxides and other reactive oxygen species (ROS). In the context of our study, we measured LPO in the sciatic nerve of rats to evaluate the extent of oxidative stress and lipid damage by quantifying the levels of malondialdehyde, which serves as the end product of LPO [226, 232]. The estimation was conducted using the thiobarbituric acid reactive substances (TBARS) assay method. In this procedure, the supernatant was combined with 20 % acetic acid, 0.8 % thio barbituric acid (TBA), and 8.1 % SDS. The mixture was thoroughly vortexed and subsequently incubated in a water bath at 95 °C for a duration of 1 h. Following cooling of the mixture, 200 µL aliquots were dispensed in duplicate into a 96-well plate, and absorbance measurements were taken at 532 nm using a multimode microplate reader [225].

7.2.5.5.3 Reduced glutathione (GSH) assay

GSH is a vital antioxidant molecule in biological systems. It plays a crucial role in protecting cells from oxidative damage by neutralizing harmful ROS and free radicals [228]. GSH levels were determined using Ellman's reagent (DTNB, 5,5′-dithiobis (2-nitrobenzoic acid)), which reacts with the reduced form of GSH present in the tissue lysate. Upon reaction, DTNB is converted into a yellow-coloured compound called TNB (thio nitro benzoic acid), which can be quantified by measuring its absorbance at 412 nm. For the assay, a desired volume of the sample was taken and mixed with phosphate buffer (pH 7.4) and 0.1 mM DTNB (prepared in pH 8.0 phosphate buffer). The mixture was thoroughly vortexed and incubated at 48–50 °C for 30 min. Subsequently, 200 µL of the sample was dispensed in duplicate into a 96-well plate, and the absorbance was measured at 412 nm using a multimode microplate reader [225].

7.2.5.5.4 Nitrite assay

Nitrite levels serves as an indicator of nitrosative stress within a cell, and elevated nitrite levels may suggest increased oxidative damage or inflammation. It was measured using the Griess reagent. In this assay, equal amounts of the tissue sample lysate and Griess reagent were mixed and incubated at room temperature for 30 min. Subsequently, the absorbance of resulting solution was measured at 540 nm using a microplate reader. The concentration of nitrite was quantified in µM/mg of tissue protein [226].

7.2.5.6 Statistical analysis

Behavioural data was analyzed using two-way ANOVA, followed by post hoc Bonferroni's multiple comparisons test. For the analysis of molecular studies data, one-way ANOVA was conducted, followed by post hoc Tukey's multiple comparison test. GraphPad Prism 8.0.2 software (Graph Pad Inc., San Diego, California, USA) was employed for performing the statistical analysis. The data were presented as mean ± SEM

(standard error mean), and a significance level of $p < 0.05$ was considered statistically significant.

7.3 Result & Discussion

7.3.1 Design rationale

The aromatization and subsequent lactone ring opening in santonin may lead to the formation of a new naproxen analogue. Naproxen is a commonly used nonsteroidal anti-inflammatory drug. Since, aromatic ring is a significant electronic feature and is considered a "privileged scaffold" in medicinal chemistry, Singh et al. synthesized a naproxen analogue (**1**) through aromatization of santonin (Figure 7.1) [221]. As **1** showed promising COX-2 inhibitory potential in earlier study, so here further optimization was carried out to improve the activity and selectivity via synthesis of different derivatives.

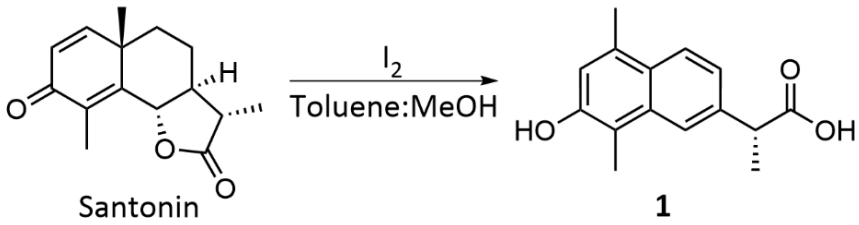

Figure 7.1 Synthetic scheme for **1** as mentioned by Singh et al.

Based on the optimized synthetic methodology of Singh et al., **1** was synthesized. It was obtained in good yield but it was noticed that some minor spot was also visible above the spot of desired compound when viewed on TLC under short UV-range (254 nm). The intensity of spot was less compared to that of desired compound but after charring with anisaldehyde-sulphuric acid reagent, a dark purple spot was visible while it was not observed in case of **1** spot. Thus, we attempted to purify and isolate this unknow compound along with **1**. After careful characterization via detailed 1D NMR, 2D NMR and Mass spectra, it was regarded as **2** and named desmotroposantonous acid, as it was the carboxylic acid derivative of desmotroposantonin only (Figure 7.2). **2** could be postulated as an intermediate in the formation of **1**. To get rid of **2** and get only **1** as single

product reaction time was increased but there was still some minor impurity of **2**. So further, there was an attempt to slightly increase the amount of iodine-catalyst. It was observed that slight increase in iodine and heating resulted in formation of some new UV-active product that was different from both **1** and **2** and also had lower polarity as visualized from TLC. The purification and further characterization of the **3** revealed it to be methyl ether and ester derivative of **1**. To further evaluate the formation of **3**, the reaction was put again and it was TLC-monitored every 2 hours, and it was found that initially **1** and **2** both were formed but they were eventually converted into **3** as a single product. Also, it was observed that no side-product was remaining and it was obtained as an almost single and major product in the reaction mixture.

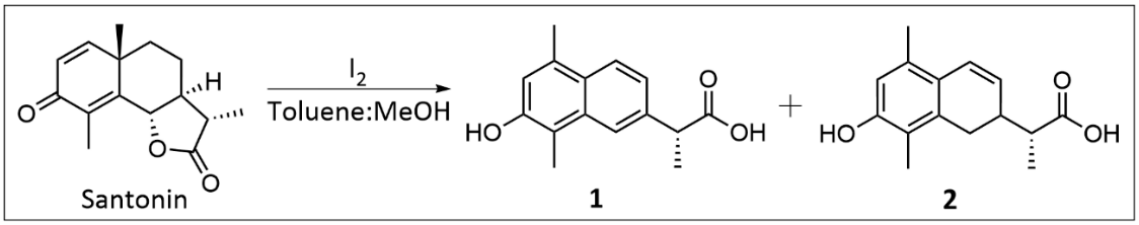

Figure 7.2 Compounds synthesized in Scheme I.

Then, to find out if the reaction underwent by changing the alcohol, we tried the reaction with ethanol instead of methanol. It was observed on TLC that a more hydrophobic product was formed and also in a slightly lesser time than that of **3**. The purification and further characterization showed it to be an ethyl derivative of **1**. Also, the product was formed almost as a single product. Subsequently, we changed alcohol (1-propanol, 1-butanol, 1-pentanol, 1-hexanol, 1-heptanol, 1-octanol, isoamylalcohol) to synthesize different types of derivatives (Figure 7.3).

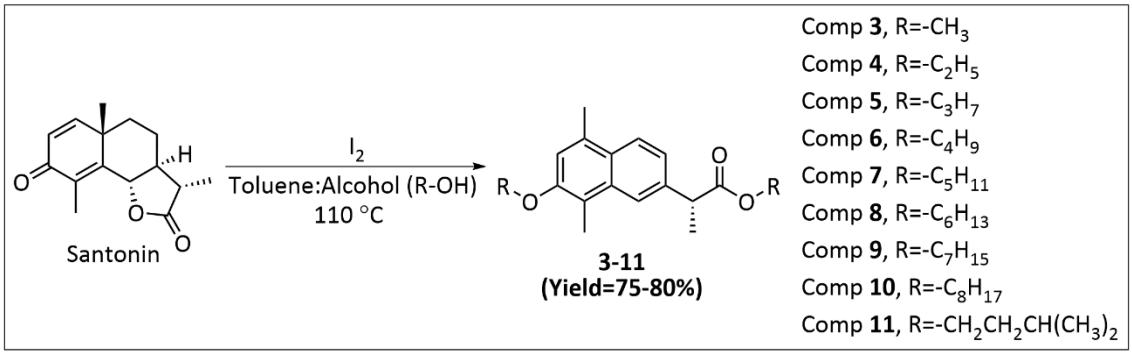

Figure 7.3 Compounds synthesized in Scheme II.

Further, attempt was made to hydrolyze the ester group to carboxylic acid to evaluate if it has influence on the activity of synthesized derivatives (Figure 7.4).

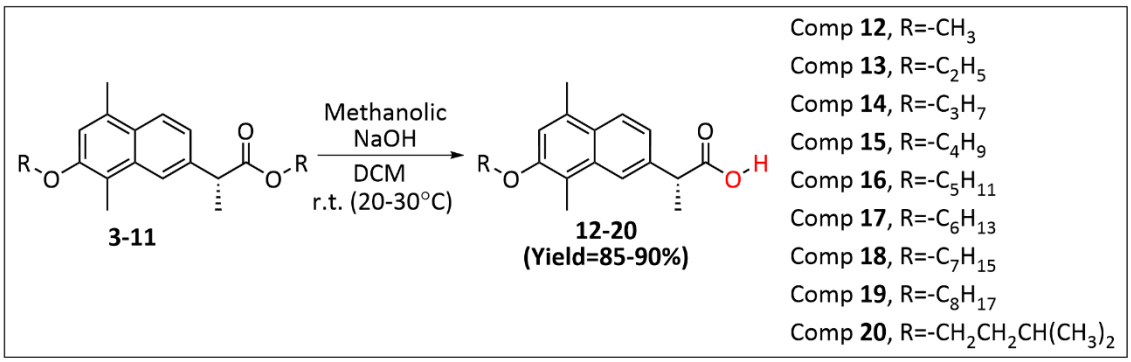

Figure 7.4 Compounds synthesized in Scheme III.

7.3.2 COX inhibition assay

The COX inhibitory potential of the synthesized compounds was evaluated using COX inhibitory screening assay. The assay was executed via commercial assay kits using naproxen (non-selective COX inhibitor) and etoricoxib (selective COX-2 inhibitor) as a control. Out of 20 synthesized compounds, **9**, **12**, and **20** exhibited good inhibitory effects against COX-2 enzyme, as shown in Table 7.1. Among **9**, **12**, and **20**, analog **12** showed potent inhibition of COX-2 enzyme compared to naproxen.

Table 7.1 *In vitro* COX-2 inhibitory activity.

Compound	COX-2 inhibition (IC_{50} in nM)
9	360.06
12	134.81
20	309.89
Naproxen	164.07
Etoricoxib	103.32

7.3.3 Docking study and MD simulation studies

Further, docking and MD simulation study was conducted for **12** to determine its binding with COX-2 proteins in *in silico* settings (Figure 7.5). The binding energy was compared against naproxen and etoricoxib. The binding energy and ligand efficiency is shown in Table 7.2.

Table 7.2 Docking score and ligand efficiency of **12**.

Ligands	COX-2	
	Binding Energy (kcal/mol)	**Ligand Efficiency (kcal/mol)**
12	-9.07	-0.477
Naproxen	-8.34	-0.491
Etoricoxib	-11.08	-0.462

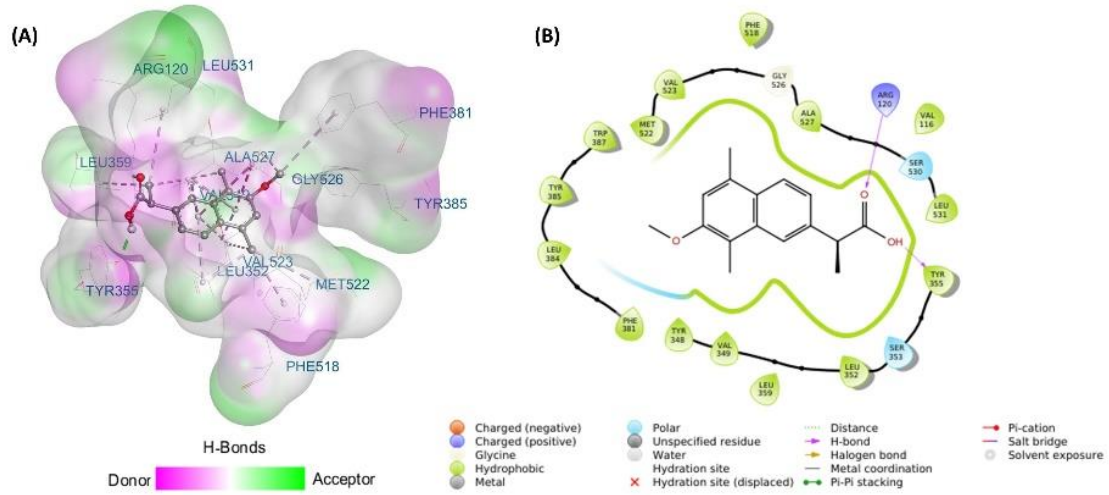

Figure 7.5 Docking interaction diagram of **12** with COX-2 protein. (**A**) 3D and (**B**) 2D interaction diagram.

In this study, the MD simulation of analog **12**-COX-2 complex was performed to determine the stability of the protein-ligand complex. The resulting trajectories were examined for RMSD, RMSF, and H-bond interactions.

The RMSD value for C-alpha backbone of COX-2 and analog **12** was calculated during a simulation that lasted 120 ns. It is clear from Figure 7.6 that the protein acquired a stable RMSD throughout the simulation. For small and globular proteins (ideal range 1-3 Å), the highest and average protein backbone RMSD for the analog **12**-COX-2 complex was 0.562 Å and 0.514 Å, respectively. The maximum and average deviations for the ligand was 0.971 Å and 0.494 Å, respectively. The RMSD of **12** was closer to protein that indicates that the ligand did not diffuse away from initial binding site. Here, L-RMSF analysis for the ligand fit on the protein and P-RMSF analysis for C-atom of COX-2 protein residues was performed. The average L-RMSF for **12** was 0.349 and the average P-RMSF for analog **12**-COX-2 complex was 0.330 Å. Furthermore, it was clear from P-RMSF that crucial residues including Arg 120, Tyr 385, and Ser 530 took part in ligand interactions and maintained a high level of stability throughout the simulation. The PL-contacts histogram was used to monitor and analyze the interactions (H-bonds, hydrophobic, ionic, and water bridges) between the COX-2 protein and **12** during the simulation run. **12** showed H-bond interactions with the residues Arg 120, Tyr 355, and Ser530 that were also seen in docking study of **12** with COX-2 protein. Additionally, it demonstrated interactions with the residues Val 349, Leu 352, Tyr 385, and Ala 527 that were hydrophobic (Figure 7.6).

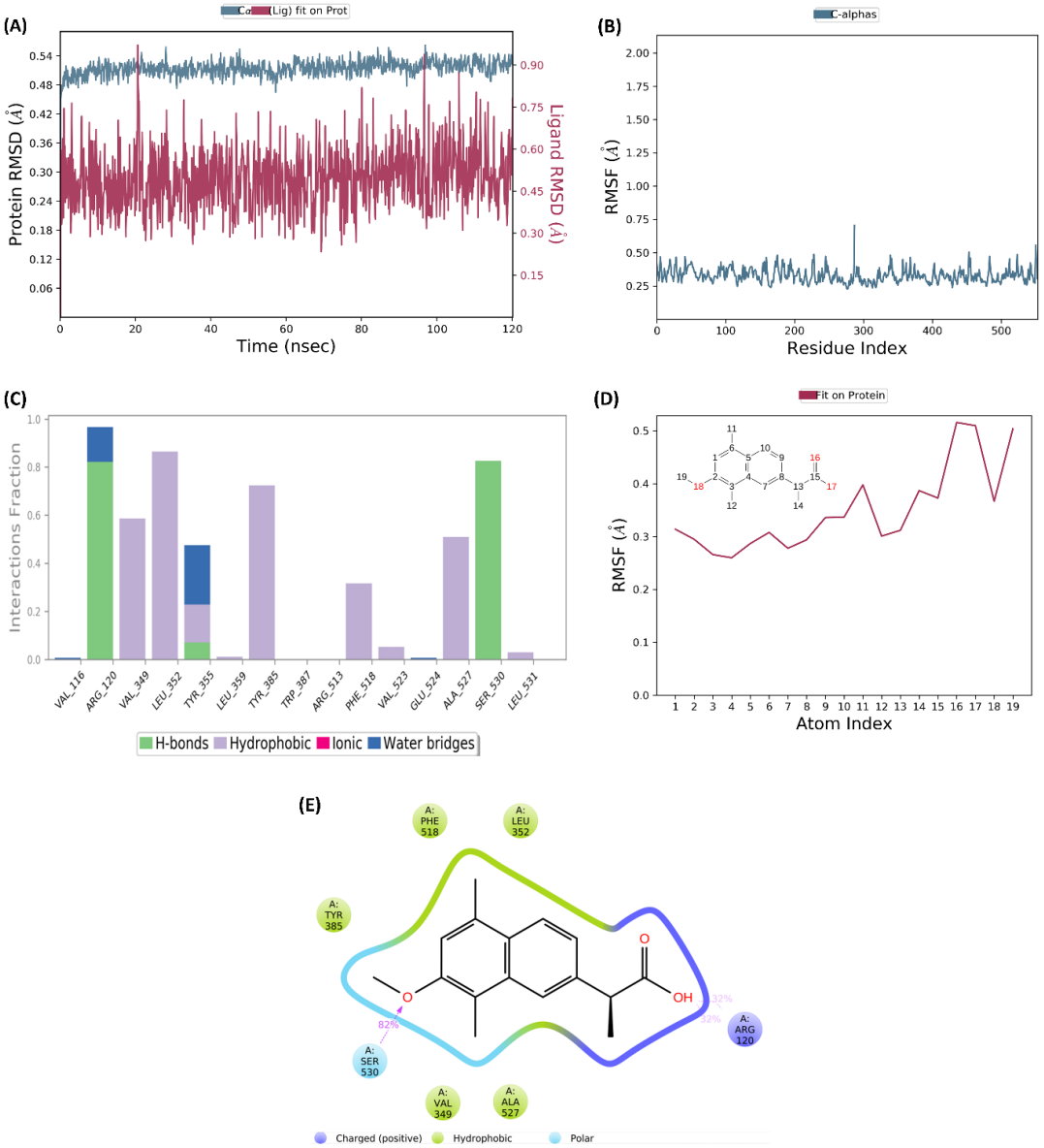

Figure 7.6 MD simulation of **12**-COX-2 complex. A) RMSD plot of protein-ligand complex, B) P-RMSF plot representing residue-wise deviation in protein, C) PL-Contacts of the protein-ligand complex during simulation run, D) L-RMSF plot representing atom wise deviation in ligand bound to protein, and E) Interactions of ligand with protein during MD run.

7.3.4 Effect of TC on CFA-induced pain-like behavior in rats

We have performed a series of pain behavioral assays such as thermal, mechanical, cold, and spontaneous ongoing pain to assess the efficacy of **12** on CFA-induced chronic pain in rats. From here TC corresponds to **12**.

7.3.4.1 TC treatment inhibits mechanical allodynia and hyperalgesia in CFA-injected rats

Mechanical allodynia and mechanical hyperalgesia are one of the prominent symptoms in patients suffering from neuropathic pain. The effect of TC on dynamic mechanical allodynia was tested using von-Frey hair test. A significant effect across the groups ($p < 0.01$) and time points ($p < 0.01$) in paw withdrawal threshold (PWT) of CFA-injected and TC-treated rats was observed in von-Frey hair test. There was a significant decrease in dynamic allodynia as ipsilateral PWT was found to be significantly decreased post-TC treatment as compared to their pre-injury baselines and naïve group rats ($p < 0.01$) (Figure 7.7). TC treatment (1, 3 and 10 mg/kg i.p) significantly restored the decreased PWT of CFA-injected rats in a dose-dependent manner. At 0.5 hr post-administration, TC 10 mg/kg ($p < 0.05$) showed a significant effect as compared to their pre-drug baselines and vehicle treated CFA-injected rats. The peak anti-allodynic effect was observed at 1 hr (3 mg/kg $p < 0.05$ and 10 mg/kg $p < 0.05$) post-TC administration which lasted for 2 hrs. Naproxen (10 mg/kg i.p) treatment also attenuated the mechanical allodynia in CFA-injected rats as compared to the vehicle treated CFA-injected rats. The contralateral PWT remains unaffected before and after, CFA-injection and treatment with TC (1, 3 and 10 mg/kg i.p) and naproxen (10 mg/kg i.p) (Figure 7.7).

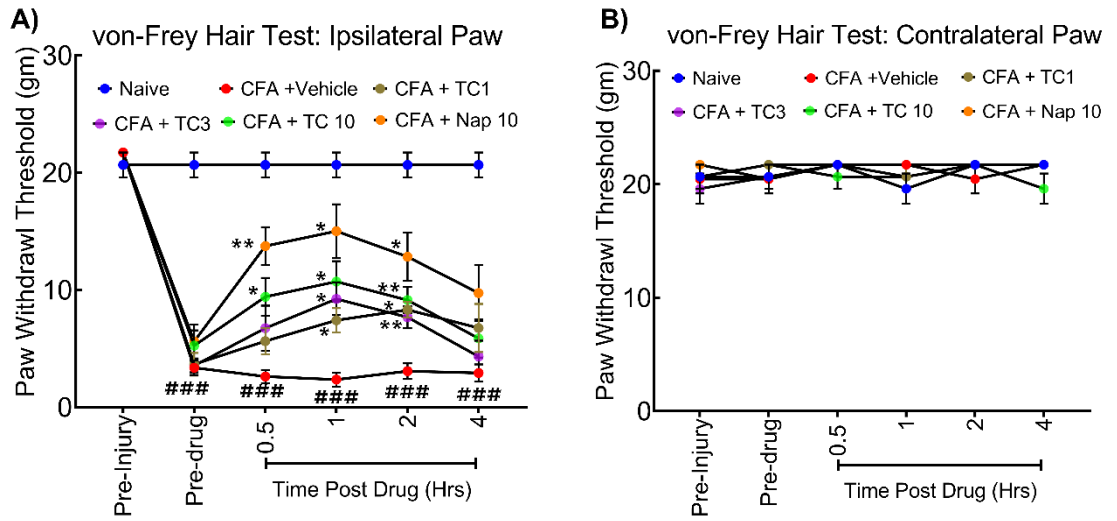

Figure 7.7 TC attenuates mechanical allodynia in CFA-injected rats. A) ipsilateral paw withdrawal threshold and B) contralateral paw withdrawal threshold. Data were expressed as Mean ± SEM and analyzed by two-way ANOVA (Bonferroni's multiple comparisons) (n=6). ### represents significance compared to the control group ($p<0.001$), * ($p<0.05$), and **($p<0.01$) represents significance compared to the CFA group. TC dose TC 1: 1mg/kg, TC 3: 3mg/kg and TC: 10mg/kg, naproxen 10 mg/kg *i.p.*

The mechanical hyperalgesia was assessed using the pinprick test. There was a significant effect observed across the groups ($p < 0.001$) in paw withdrawal frequency (PWF) of CFA-injected rats and TC-treated rats. CFA-injected rats showed a significant ($p < 0.001$) increase in ipsilateral PWF as compared to their pre-injury baselines and naïve rats. TC treatment significantly decreased the PWF of CFA-injected rats at 0.5 hr (1 mg/kg, 3 mg/kg, and 10 mg/kg $p < 0.001$) that persisted for 4 hr (3 mg/kg and 10 mg/kg $p < 0.001$) post drug administration as compared to the vehicle treated group. However, 1 mg/kg TC did not produce significant inhibition of mechanical hyperalgesia specifically at 2 hr and 4 hr post-drug administration (Figure 7.8). Naproxen (10 mg/kg i.p) treated CFA-injected rats showed a significant increase in PWF at different time points as compared to the vehicle treated CFA-injected rats. There was no significant effect observed in contralateral PWF before and after CFA-induced injury and treatment with TC (1, 3 and 10 mg/kg i.p) and naproxen (10 mg/kg i.p) (Figure 7.8).

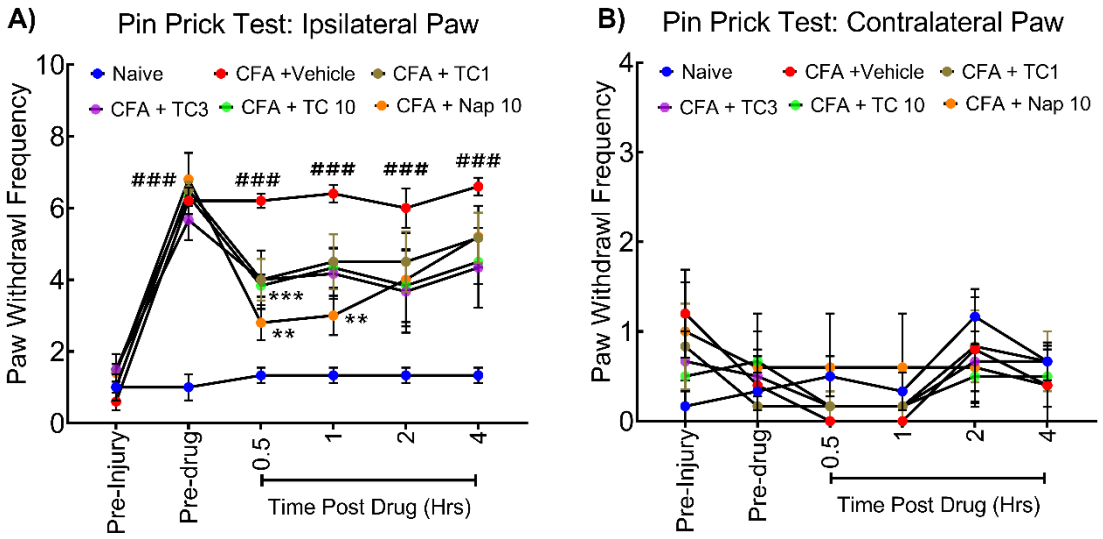

Figure 7.8 TC attenuates mechanical hyperalgesia in CFA-injected rats. A) ipsilateral paw withdrawal frequency and B) contralateral paw withdrawal frequency. Data were expressed as Mean ± SEM and analyzed by two-way ANOVA (Bonferroni's multiple comparison) (n=6). ### represents significance compared to the control group ($p<0.001$), **($p<0.01$) and *** ($p<0.001$) represents significance compared to the CFA group. TC dose TC 1: 1mg/kg, TC 3: 3mg/kg and TC: 10mg/kg, naproxen 10 mg/kg *i.p.*

7.3.4.2 TC treatment attenuates thermal hyperalgesia in CFA-injected rats

CFA-induced injury led to significant decrease in ipsilateral paw withdrawal latencies (PWL) of CFA-injected rats ($p < 0.01$) as compared to their pre injury baselines and healthy naïve group (Figure 7.9). TC treatment (3 and 10 mg/kg i.p) significantly attenuated the thermal hyperalgesia as evident by an increase in PWL of CFA-injected rats as compared to their pre-drug baselines. An increase in latency trend was observed at 30 min post-TC administration which was absent in vehicle treated CFA-injected rats (Figure 7.9). The significant and peak effect of TC started at 1 hr post-administration i.e 3 mg/kg ($p < 0.05$) and 10 mg/kg ($p < 0.01$) that lasted up to 2 hr followed by a decline in the effect of TC. However, 1 mg/kg dose did not show significant effect at 4 hr post-drug administration in restoring CFA-induced decreased PWL. A significant effect on thermal hyperalgesia was observed across the groups ($p < 0.01$) and time points ($p < 0.01$). The standard drug naproxen (10 mg/kg i.p) showed significant effect at 1 hr post-

administration ($p < 0.01$) and 2 hr ($p < 0.01$), and the effect lasted for the 4-hr post-administration ($p < 0.01$) as compared to the vehicle treated CFA-injected rats. Moreover, contralateral PWL of CFA-injected rats was not altered before and after, CFA-injection and drug treatments (TC and naproxen) (Figure 7.9).

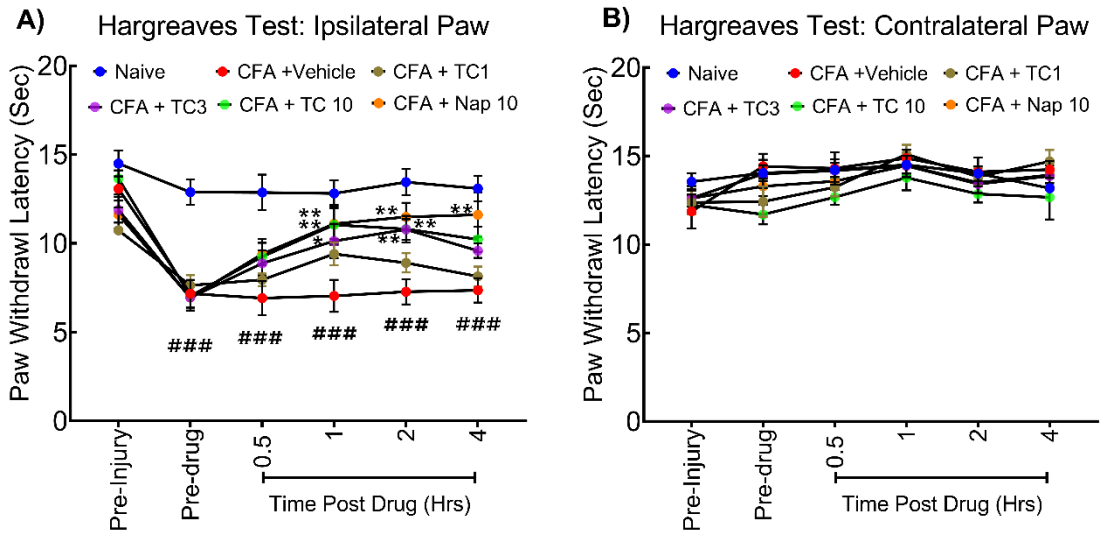

Figure 7.9 TC attenuates thermal hyperalgesia in CFA-injected rats. A) ipsilateral paw withdrawal latency and B) contralateral paw withdrawal latency. Data were expressed as Mean ± SEM and analyzed by two-way ANOVA (Bonferroni's multiple comparison) (n=6). ### represents significance compared to the control group ($p<0.001$), * ($p<0.05$), and **($p<0.01$) represents significance compared to the CFA group. TC dose TC 1: 1mg/kg, TC 3: 3mg/kg and TC: 10mg/kg, naproxen 10 mg/kg *i.p.*

7.3.4.3 TC attenuates cold allodynia and cold hyperalgesia in CFA-injected rats

Hypersensitivity induced by non-noxious and noxious cold stimuli is notable trait among neuropathic pain patient. Here we investigated the effect of TC on cold allodynia and cold hyperalgesia in CFA-injected rats. Acetone drop test was used to evaluate the non-noxious stimuli evoked cold allodynia in CFA-injected rats. CFA-induced injury has increased the response score to non-noxious cold stimuli in ipsilateral paw as compared to the respective pre-injury baselines and naïve rats. TC treatment significantly decreased the response score at 1 hr (10 mg/kg, $p < 0.05$) post administration as compared to their respective pre-treatment baselines and vehicle treated CFA-injected rats (Figure 7.10).

Naproxen (10 mg/kg i.p) also decreased the cold allodynia evident by a significant decrease in ipsilateral paw response score at 1 hr ($p < 0.05$) post administration as compared to the vehicle treated CFA-injected rats.

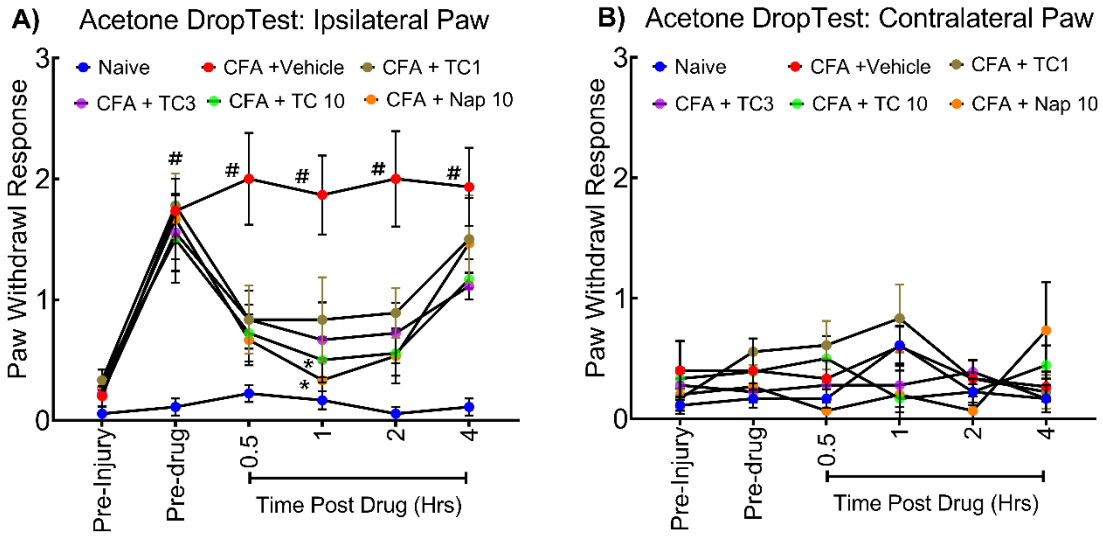

Figure 7.10 TC attenuates cold allodynia in CFA-injected rats. A) ipsilateral paw withdrawal responses and B) contralateral paw withdrawal responses. Data were expressed as Mean ± SEM and analyzed by two-way ANOVA (Bonferroni's multiple comparison) (n=6). # represents significance compared to the control group ($p<0.05$), and * ($p<0.05$), represents significance compared to the CFA group. TC dose TC 1: 1mg/kg, TC 3: 3mg/kg and TC: 10mg/kg, naproxen 10 mg/kg *i.p.*

Further we tested the effect of TC on noxious cold stimuli induced cold hyperalgesia. It was found that CFA-induced injury has increased the number of ipsilateral paw lifts significantly in presence of noxious cold stimulus as compared to their pre-injury baselines and naïve rats ($p < 0.001$) (Figure 7.11). There was a significant reduction in number of paw lifts post TC administration at 1 hr (10 mg/kg, $p < 0.05$) and 2 hr (10 mg/kg, $p < 0.05$) as compared to the vehicle treated CFA-injured rats. Naproxen (10 mg/kg i.p) also significantly decreased the number of ipsilateral paw lifts as compared to the CFA-injured rats post 0.5 hr ($p < 0.05$), 1 hr ($p < 0.01$), and 2 hr ($p < 0.01$) of administration. However, CFA-induced injury and drug treatments did not show a

significant effect on allodynic response score and noxious stimuli induced cold hypersensitivity in contralateral paw of rats as compared to their respective pre-injury and pre-drug baselines (Figure 7.11).

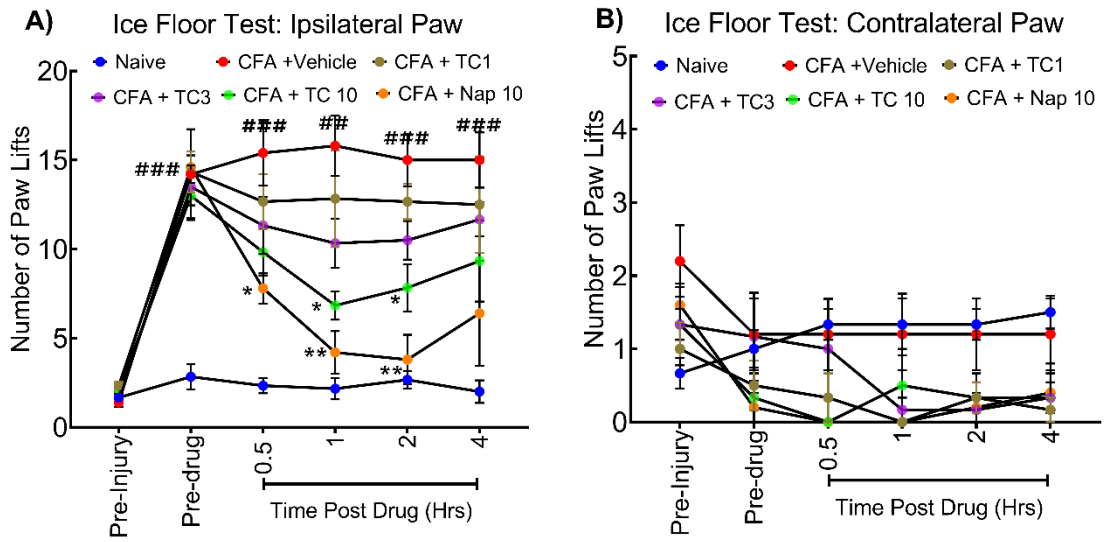

Figure 7.11 TC attenuates cold hyperalgesia in CFA-injected rats. A) ipsilateral paw lifts and B) contralateral paw lifts. Data were expressed as Mean ± SEM and analyzed by two-way ANOVA (Bonferroni's multiple comparison) (n=6). ## ($p<0.01$), ### ($p<0.001$) represents significance compared to the control group, *($p<0.05$) and **($p<0.01$) represents significance compared to the CFA group. TC dose TC 1: 1mg/kg, TC 3: 3mg/kg and TC: 10mg/kg, naproxen 10 mg/kg *i.p.*

7.3.4.4 TC does not affect locomotor or exploratory activity of CFA-injected rats

Further we investigated the effects of TC on motor coordination and locomotor activity of rats. In the open field test, we observed that TC (10 mg/kg i.p) treatment did not alter the exploratory or locomotor behavior of CFA-injured rats (Figure 7.12) as there was no significant change in the total distance travelled of TC treated CFA-injured rats as compared to the naïve rats. Moreover, treatment with naproxen (10 mg/kg i.p) also produced no observable effects on the locomotor behavior of CFA-injured rats. In rotarod test also, TC (10 mg/kg i.p) as well as naproxen (10 mg/kg i.p) treatment showed no significant change in time spent on rod as compared to the CFA-injured rats (Figure 7.12).

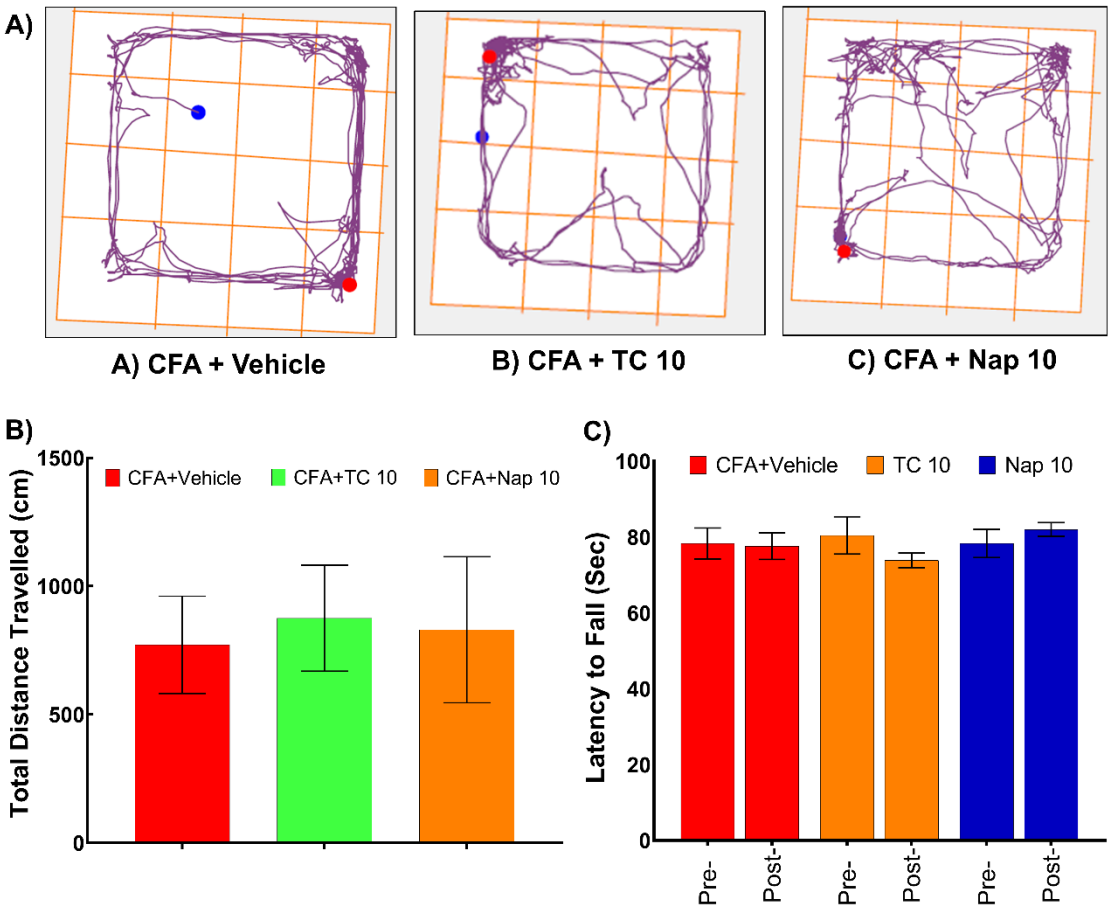

Figure 7.12 Effect of TC on locomotor activity and motor coordination in CFA-injected rats. (A) TC did not affect the locomotor activity of CFA-injected rats- Open-Field Test a) Track Images b) Total distance travelled. (B) TC did not affect the Motor Coordination of CFA-injected rats- Rota rod test. Data were expressed as Mean ± SEM and analyzed by two-way ANOVA (Bonferroni's multiple comparison) (n=6). TC dose TC 1: 1mg/kg, TC 3: 3mg/kg and TC: 10mg/kg, naproxen 10 mg/kg *i.p.* Data was nonsignificant compared to the vehicle group.

7.3.4.5 TC attenuates oxidative stress in sciatic nerve of CFA-injected rats

Generation of ROS and RNS are important features of chronic inflammation. So, we evaluated the effect of TC on levels of various oxidative markers and antioxidant enzymes. We utilized spectrophotometric analysis techniques to evaluate the biochemical alterations occurring in the sciatic nerve of rats, following CFA-injury and subsequent treatment with TC. The statistical analysis showed a significant influence on the levels of GSH, MDA, and nitrite across the different treatments. The level of antioxidant GSH was

decreased ($p < 0.001$) after CFA administration whereas nitrite and MDA levels were significantly increased ($p < 0.001$). Different doses of TC treatment restored the levels of GSH (5 mg/kg, $p < 0.05$ & 10 mg/kg, $p < 0.01$) and alleviated levels of nitrite (10 mg/kg, $p < 0.05$) and MDA (5 mg/kg, $p < 0.05$ & 10 mg/kg, $p < 0.01$) (Figure 7.13). However, the dose of 5 mg/kg TC does not have significant effect in attenuating nitrite levels Further, naproxen treatment also alleviated the oxido-nitrosative stress by decreasing the levels of nitrite ($p < 0.01$) and MDA ($p < 0.001$), while restoring the GSH levels ($p < 0.05$) in sciatic nerve of neuropathic rats (Figure 7.13).

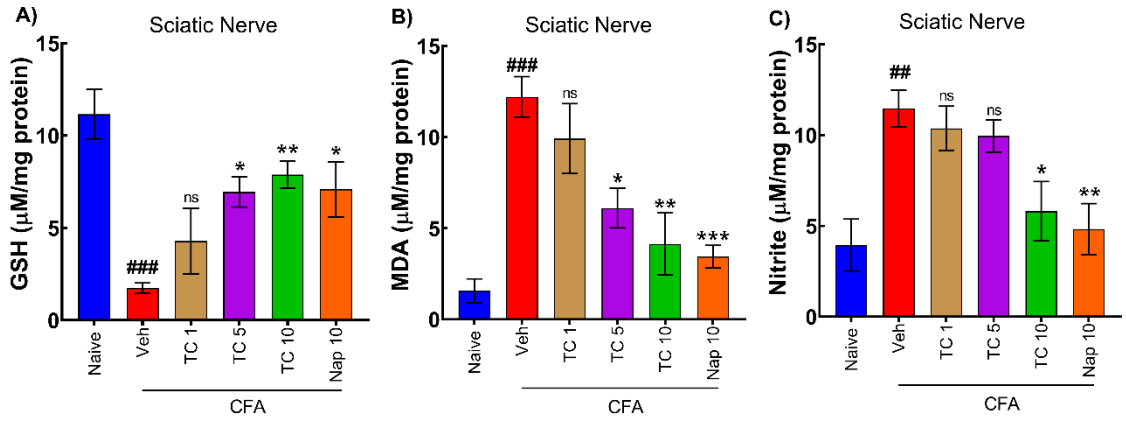

Figure 7.13 TC attenuates oxidative stress in sciatic nerve of CFA-injected rats. (A) GSH levels: TC (5 and 10 mg/kg i.p.) and naproxen (10 mg/kg i.p.) administration restored GSH levels in CFA-treated rat sciatic nerves compared to vehicle-treated rats. (B) MDA levels: CFA-treated rats exhibited elevated MDA levels, reduced significantly by TC (5 and 10 mg/kg i.p.) and naproxen (10 mg/kg i.p.). Notably, the 1 mg/kg i.p. TC dose did not impact MDA levels. (C) Nitrite levels: CFA-induced nitrite elevation was significantly mitigated by TC (10 mg/kg i.p.) and naproxen (10 mg/kg i.p.), with no significant effect observed at the 1 and 5 mg/kg i.p. dose of TC. Data expressed as Mean ± SEM (n=4). ## ($p<0.01$), ### ($p<0.001$) represents significance compared to the control group, *($p<0.05$), **($p<0.01$) and *** ($p<0.001$) represents significance compared to the CFA group. ns represents nonsignificant compared to the vehicle group. TC dose TC 1: 1mg/kg, TC 3: 3mg/kg and TC: 10mg/kg, naproxen 10 mg/kg *i.p.*

7.4 Conclusion

The semi-synthetic modification performed on the lead santonin obtained from network pharmacology approach, resulted in twenty derivatives. The santonin analogs synthesized using molecular iodine as catalyst were structurally similar to naproxen, a NSAID. The *in vitro* COX enzyme inhibition assay of synthesized santonin derivatives, unveiled analog **12** with potent COX-2 inhibitory potential as well as COX-2 selectivity. Later, *in vivo* anti-inflammatory potential of **12** on CFA model of inflammation demonstrated that the synthesized analog **12** effectively reduced both provoked and spontaneous pain in an animal model of CFA-induced peripheral pain. The inhibition of COX-2 using TC also reduced CFA-induced pain hypersensitivity in rats by disrupting prostaglandin signaling, thereby inhibiting inflammatory and oxido-nitrosative processes. It is noteworthy that TC administration did not cause sedation or motor coordination issues. Developing new NSAID pain relievers targeting selective inhibition could offer safer and more effective treatments for chronic pain. Hence, TC may represent a promising and safer alternative to naproxen for alleviating pain in patients with chronic inflammation.